# Optical pulse propagation in dynamic Fabry–Perot resonators

**Yuzhe Xiao,[1,*] Drew N. Maywar,[2] and Govind P. Agrawal[1]**

[1]*The Institute of Optics, University of Rochester, Rochester, New York 14627, USA*
[2]*Electrical, Computer, and Telecommunications Engineering Technology, Rochester Institute of Technology, Rochester, New York 14623, USA*
**Corresponding author: yuxiao@optics.rochester.edu*

Received April 6, 2011; accepted May 16, 2011;
posted May 24, 2011 (Doc. ID 145385); published June 14, 2011

We present a simple and intuitive model based on the impulse response of linear electrical systems for describing the propagation of optical pulses through a dynamic Fabry–Perot resonator whose refractive index changes with time. Our model shows that the adiabatic wavelength conversion process in resonators results from a scaling of the round-trip time with index changes. For pulses longer than the cavity round-trip time, we find that more energy can be transferred to the new wavelength when the input pulses are slightly detuned from the cavity resonance and the refractive index does not change too rapidly. In fact, the optimum duration of index changes scales with the photon lifetime of the resonator. We describe the evolution of the shape and spectrum of picosecond pulses inside a resonator under a variety of input conditions and with the magnitude and duration of index variations. We also apply our general theory to the case of pulses whose widths are shorter than the round-trip time and derive an analytical expression for the output field under quite general conditions. This analysis reveals a shifting of the spectral comb as well as compression of the temporal pulse train that depends on the both the magnitude and sign of the index change. Our results should find applications in the area of optical signal processing using resonant photonic structures. 

*OCIS codes:* 130.7405, 320.5540, 350.4238.

## 1. INTRODUCTION

In recent years, new kinds of optical resonators, based on silicon microrings and photonic crystals, are being used to make optical devices with numerous potential applications. An example is provided by the recently discovered phenomenon of *adiabatic wavelength conversion* (AWC) occurring inside an optical resonator [1–6] whose refractive index is forced to change with time while an optical pulse is transmitted through it. In contrast to conventional static resonators, it is common to think of such a resonator as being dynamic. This paper focuses on such dynamic resonators. Although they can have different configurations, their properties can be studied by considering a generic Fabry–Perot (FP) resonator. Historically, dynamic FP resonators with moving mirrors were first considered during the 1960s in the context of mode locking [7]. Such resonators have continued to attract attention and have found applications in the fields of spectroscopy and interferometry [8–12].

In this paper, we consider optical resonators whose refractive index is changed in a dynamic fashion. In the case of AWC, it was found that a pulse can shift its wavelength even when the dynamic resonator contains a *linear optical medium*. Numerical methods based on the finite-difference time-domain solutions of Maxwell's equations are often used to understand the AWC phenomenon [3,6]. A modal approach has also been used to study this effect [13]. Here, we present a new approach based on the theory of linear electrical systems described in terms of an impulse response function. In particular, we extend our analysis of [14] carried out for single-pass traveling-wave systems to optical resonators whose refractive index changes with time. The impulse response function of a dynamic FP resonator is derived in Section 2, where we also show that our approach is consistent with the usual frequency-domain approach in the special case of static resonators. Section 3 focuses on the case of instantaneous changes in the refractive index when a short optical pulse is injected into the resonator. Our results agree with previously known changes in the central wavelength and pulse energy. In addition, we show that AWC is accompanied with changes in the temporal width, spectral width, and peak intensity of optical pulses. In Section 4 we consider the more general case of a relatively long pulse transmitted through a dynamic resonator. Not only does our method correctly reproduce the magnitude of the AWC peak in the frequency domain, it also allows us to study the temporal and spectral evolutions of optical pulse associated with the AWC phenomenon. Section 5 is devoted to studying the impact of externally controllable parameters such as the magnitude of index change, the speed with which this change is implemented, and the detuning of the input pulse. The main results are summarized in the final, concluding section.

## 2. IMPULSE RESPONSE FUNCTION OF LINEAR SYSTEMS

A linear system is fully characterized by its impulse response function. More specifically, the output signal $E_{\text{out}}(t)$ is related to the input signal $E_{\text{in}}(t)$ through

$$E_{\text{out}}(t) = \int_{-\infty}^{\infty} h(t,t')E_{\text{in}}(t')\mathrm{d}t', \tag{1}$$

where $h(t,t')$ is the impulse response function. In the case of an optical pulse transmitted through a dielectric slab of length

 

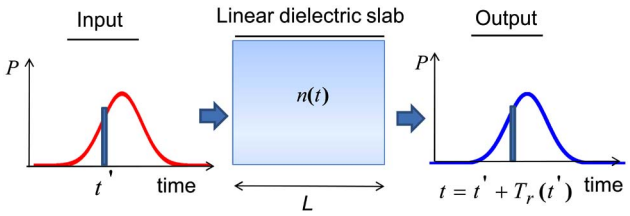


Fig. 1. (Color online) Schematic illustration of pulse propagation through a dynamic optical medium with refractive index $n(t)$. Each temporal slice of the input pulse is delayed by a time-dependent transit time $T_r(t')$.

$L$ (see Fig. 1), $E_{\text{in}}(t)$ and $E_{\text{out}}(t)$ correspond to the electric fields associated with an electromagnetic field at the input and output ends of the slab located at $z = 0$ and $z = L$, respectively.

If the refractive index $n$ of this dielectric slab remains constant with time, it is a time-invariant linear system. In this case, $h(t, t')$ becomes a function of a single variable $h(t - t')$; it is useful to work in the spectral domain, because Eq. (1) takes the simple form $\tilde{E}_{\text{out}}(\omega) = H(\omega)\tilde{E}_{\text{in}}(\omega)$, where a tilde represents the Fourier transform and $H(\omega)$ is the Fourier transform of $h(t - t')$. Clearly, a time-invariant system acts as an optical filter. Because a spectral-domain approach is not useful for time-variant systems, we do not use it in this paper and work directly in the time domain. If we assume for simplicity that the dielectric slab responds instantaneously to the optical field, both the loss and dispersion of the medium can be ignored, and $n$ can be treated as a real constant over the entire pulse bandwidth. Because the optical pulse remains unchanged when transmitted through such a slab, except for being delayed by the transit time $T_r = nL/c$, it is easy to see that $E_{\text{out}}(t) = E_{\text{in}}(t - T_r)$ if the impulse response function is given by $h(t - t') = \delta(t - t' - T_r)$.

The question is what happens in a dynamic optical system whose refractive index $n(t)$ is allowed to change with time while the pulse is propagating through it. Figure 1 shows the situation graphically. It is useful to divide the pulse into temporal slices. In the dynamic case, the transit time is not the same for all pulse slices but depends on details of how $n(t)$ changes with time. It turns out that the impulse response function for a dynamic linear system has the general form [14]

$$h(t, t') = \delta[t - t' - T_r(t')], \tag{2}$$

where $T_r(t')$ is the transit time associated with a specific temporal slice of the input pulse, and it can be determined by the following simple relation:

$$\int_{t'}^{t'+T_r(t')} [c/n(\tau)]\mathrm{d}\tau = L. \tag{3}$$

This form was used in [14] to discuss temporal and spectral changes occurring when an optical pulse is transmitted through a dynamic traveling-wave slab.

We now convert a dielectric slab into an FP resonator by assuming that its two facets located at $z = 0$ and $z = L$ act as mirrors of reflectivity $R$. Because the optical pulse is now forced to make multiple passes within the resonator, the output field is *not* in the form of a single pulse. Rather, as seen in Fig. 2, it is composed of a sequence of output fields of decreasing amplitudes resulting from successive passes within the

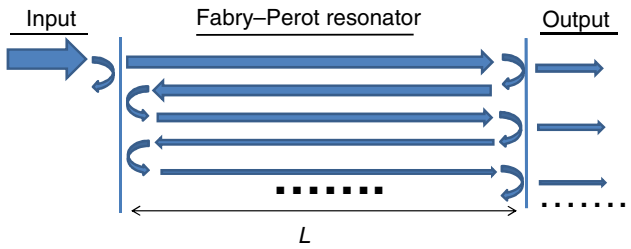


Fig. 2. (Color online) Schematic illustration of multiple round trips within an FP resonator.

resonator. The impulse response function of an FP resonator is then given by

$$h(t, t') = (1 - R)\sum_{m=0}^{\infty} R^m \delta[t - t' - T_m(t')], \tag{4}$$

where $m = 0, 1, 2\ldots$ for successive round trips within the resonator. The quantity $T_m(t')$ is the transit time for the pulse slice that enters the resonator at time $t'$ and leaves after $m$ round trips. It is readily obtained from Eq. (3) by replacing $L$ with $(2m + 1)L$, where $L$ is the physical length of the resonator. Equation (1) together with Eq. (4) fully characterize a dynamic FP resonator for an arbitrary functional form of $n(t)$ and an arbitrary input field.

Before considering the dynamic situation, we apply Eq. (3) to a static FP resonator with a constant refractive index $n_0$. It follows from Eqs. (1)–(4) that the impulse response function of a static FP resonator is given by

$$h(t - t') = (1 - R)\sum_{m=0}^{\infty} R^m \delta[t - t' - (2m + 1)T_0/2], \tag{5}$$

where $T_0 = 2n_0L/c$ is the round-trip time. Taking the Fourier transform of Eq. (5) and summing up the resulting series, we obtain the frequency-domain transfer function in the form

$$H(\omega) = (1 - R)e^{i\omega T_0/2}/(1 - Re^{i\omega T_0}). \tag{6}$$

This is identical to the well-known transfer function of static FP resonators [15]. This agreement between the time-domain and frequency-domain approaches in the time-invariant case was expected on physical grounds. In the following sections, we focus on several time-variant cases.

## 3. PULSES THAT ARE SHORT COMPARED TO ROUND-TRIP TIME

In this section we consider the case in which the input pulses are short compared to the round-trip time. To begin with, the refractive index is assumed to change instantaneously from its initial value of $n_1$ to $n_2$ at change time $T_c$ and to remain at $n_2$ after that, i.e.,

$$n(t) = \begin{cases} n_1 & (t < T_c) \\ n_2 & (t \geq T_c) \end{cases}. \tag{7}$$

If the optical pulse enters the resonator after $T_c$, it does not experience the refractive index change and the resonator is effectively static. We are only interested in pulses that enter the resonator before the refractive index changes.

The time $T_m(t')$ appearing in Eq. (4) can be calculated analytically for this index-change model by writing the integral in Eq. (3) in the form

$$\int_{t'}^{T_c} \frac{c}{n_1} d\tau + \int_{T_c}^{t'+T_m(t')} \frac{c}{n_2} d\tau = (2m+1)L. \tag{8}$$

Both integrals can be performed easily, and the result is

$$T_m(t') = (1-s)t'/s + T_{\text{em}}, \tag{9}$$

where $s = n_1/n_2$ is the relative index change and $T_{\text{em}}$ is defined as

$$T_{\text{em}} = (2m+1)n_2L/c + (1-1/s)T_c. \tag{10}$$

If there is no refractive-index change (the pulse leaves before the change time $T_c$), then $n_2 = n_1$, $s = 1$, and $T_{\text{em}}$ is reduced to the value of $(2m+1)n_1L/c$ expected on physical grounds. Compared to the time-invariant case, the most important feature of Eq. (9) is a rescaling of the slice transit time $t'$ to $t'/s$. As we shall see later, this scaling affects the optical pulse in several different ways.

Once we know $T_m(t')$, the transfer function $h(t,t')$ is known from Eq. (4). By substituting $h(t,t')$ into Eq. (1), we can obtain the output field in the form

$$E_{\text{out}}(t) = (1-R)\sum_{m=0}^{\infty} R^m [sE_{\text{in}}(st - sT_{\text{em}})]. \tag{11}$$

Equation (11) shows that the effect of changing the medium's refractive index in a dynamic fashion manifests through a simple scaling parameter $s = n_1/n_2$ that only depends on the ratio of the initial and final values of the refractive index. As will be seen later, this scaling leads to pulse compression or broadening, depending on whether $s > 1$ or $s < 1$. Notice that the amplitude is also altered by the same factor $s$.

As an illustration, we apply the general analysis to the specific case of a Gaussian input pulse with the carrier frequency $\omega_1$. The input field is then given by

$$E_{\text{in}}(t) = E_0 \exp[-t^2/(2T_0^2) - i\omega_1 t], \tag{12}$$

where the pulse width $T_0 < n_1L/c$ so that the entire pulse can fit within the resonator. To make our calculation relevant for silicon microrings, we consider a relatively short FP resonator with $L = 10\,\mu$m, $n_1 = 3.5$, and $R = 0.8$. Because the round-trip time is only 233 fs, we choose $T_0 = 60$ fs. The carrier frequency of the pulse is chosen to be 192.86 THz so that it coincides with one of the cavity modes and corresponds to a wavelength of 1555.56 nm.

Figure 3 shows shapes and spectra of the output pulse in two cases in which the refractive index of the resonator medium increases (blue solid curves) or decreases (red dashed curves) by 5% from its initial value of 3.5 at $T_c = 0.25$ ps. The input pulse and spectrum are also shown for comparison (black dotted–dashed curves). The multiple pulses seen in Fig. 3(a) result from the sum in Eq. (11); index changes not only shift the exit time of subpulses but also lead to changes in their widths and amplitudes. The changes in amplitude and width of the subpulses are consistent with the result of [14]. As

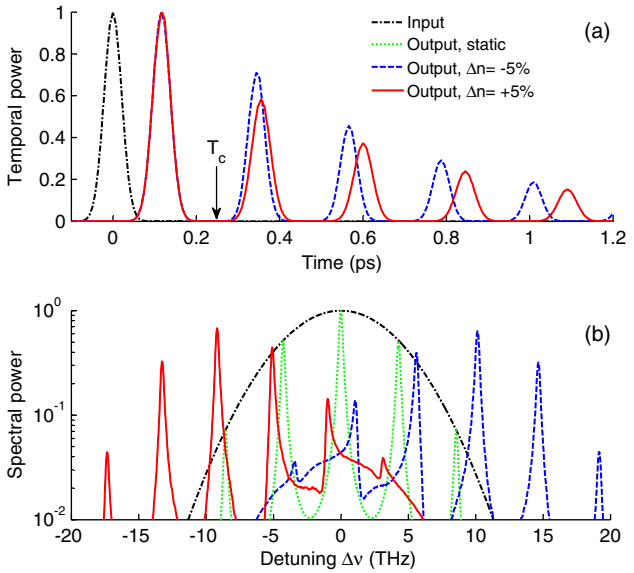


Fig. 3. (Color online) Short-pulse (60 fs) propagation for an instantaneous change in the refractive index of −5% (dashed blue curve) and +5% (solid red curve) at time $T_c = 250$ fs. The round-trip time is 233 fs. Detuning $\Delta\nu$ is defined as $\nu - \nu_0$, where $\nu_0$ is the input frequency. (a) The index change alters the width, amplitude, and delay of temporal pulses after $T_c$. (b) The index change shifts the comblike input spectrum (green dotted curve) to higher (+5%) and lower (−5%) frequencies at the FP output.

seen in Fig. 3(b), the output spectrum is affected much more (compare to the pulse shape) by index changes. The ultrashort input pulse has a broad enough spectrum that it excites five cavity modes in both the static (dotted green curve) and dynamic (solid blue and dashed red curves) cases. However, spectral peaks exhibit a blue- or redshift of about 10 THz in the two dynamic cases. The shifted peaks correspond to new cavity mode frequencies $\nu_k = kc/(2n_2L)$, where $k$ is an integer, after the refractive index is changed from $n_1$ to $n_2$.

Although spectral shifts resulting from AWC in dynamic resonators are well known [3–5], it has not been realized that the spectral shape also changes considerably. As seen in Fig. 3(b), the output spectrum exhibits considerable asymmetry. This asymmetry is due to the asymmetric nature of the index-change process with respect to the pulse center. More precisely, the refractive index is changed after the pulse has already entered the resonator and a part of its energy has already leaked out of the resonator. This feature implies that different parts of the temporal output should have different spectral contents (i.e., the pulse is chirped). A spectrogram is often used to display time-dependent spectral changes [16]. It is constructed by using a sampling function $W(t,\tau)$ that selects different temporal pulse slices. We calculate it using

$$S(\omega,\tau) = \left| \int_{-\infty}^{\infty} W(t,\tau) E_{\text{out}}(t) e^{i\omega t} dt \right|^2. \tag{13}$$

Figure 4 shows the spectrogram calculated using a Gaussian-shape sampling function in the case of a −5% reduction in the refractive index. One can clearly see that the first output field ($m = 0$ term) is centered at the original frequency, because the index has not yet been changed, while the remaining output fields ($m > 0$) are all centered at the frequency shifted by about 10 THz, because they exit the resonator after the index has been changed.

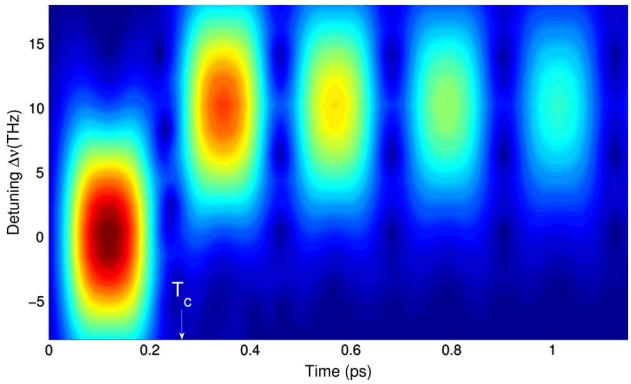


Fig. 4. (Color online) Spectrogram for the short-pulse case shown in Fig. 3 for $\Delta n = -5\%$ at time $T_c = 250$ fs. A shift of about 10 THz in the carrier frequency of the pulse is clearly seen after the index change at time $T_c$.

In constructing Figs. 3 and 4, the refractive index was changed by 5%, a relatively large amount that is presently hard to realize experimentally, where the index changes are often produced by injecting free carriers into the mode volume within a silicon waveguide [4]. In practice, index changes are typically below 0.5%. Our results show that changes in the time domain are relatively minor and barely noticeable for such small index changes. In the spectral domain, although the spectral shifts are much lower (<1 THz), the output spectrum remains asymmetric and exhibits features that should be measurable experimentally.

One interesting point to note is that the response of a dynamic FP resonator does not depend on the carrier frequency detuning from the cavity resonance for short pulses. This is readily seen from our time-domain approach. The transmitted pulse is a sequence of subpulses that are separated temporally by the resonator round-trip time. If the input pulse width is much smaller than this round-trip time, individual subpulses are separated far enough that there is hardly any overlap among them. In this case, the subpulse shape does not depend on the pulse's carrier frequency. This behavior is also understandable in the frequency domain. The input pulse spectrum is filtered by a comblike transfer function of the resonator. If the pulse is short enough, its spectrum covers several peaks of this comb. In this situation, the relative location of the carrier frequency with respect to the cavity resonances has little effect on the output pulse shape.

## 4. PULSES THAT ARE LONG COMPARED TO ROUND-TRIP TIME

In this section we focus on a more practical situation where input pulses are considerably wider than the resonator round-trip time. Different from the short-pulse case, such a long pulse cannot be fully confined within the resonator, and only a part of the pulse that is inside the resonator experiences the refractive-index change. Moreover, some parts of the pulse only experience a portion of the index change. As a result, the scaling factor $s$ and the effective time $T_{\mathrm{em}}$ appearing in Eq. (10) now themselves become time dependent. In this situation, it is not possible to obtain an analytic expression for the output field similar to that obtained in Eq. (11) for short pulses.

To investigate AWC process in dynamic resonators, numerical calculations are performed for a 10 $\mu$m long FP resonator

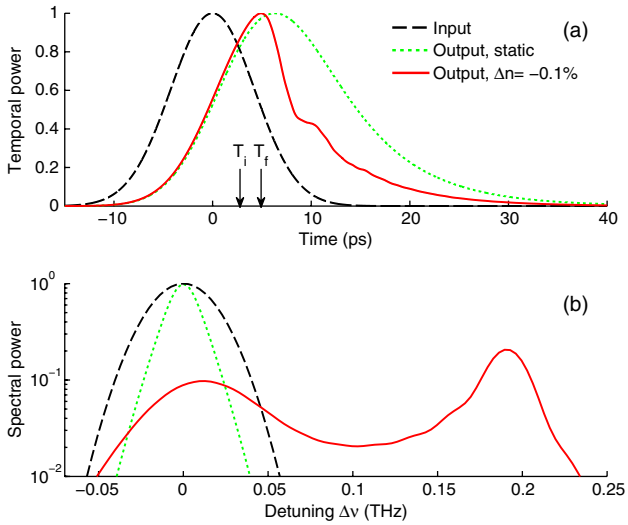


Fig. 5. (Color online) Long-pulse (10 ps) propagation for a linear change in refractive index of −0.1% (solid red curve) between $T_i = 3$ ps and $T_f = 6$ ps (marked by arrows). The round-trip time of the resonator is 0.23 ps. (a) The index change advances the output peak and produces a long tail with a kneelike feature. (b) The output spectrum shows two spectral peaks corresponding to the original and shifted cavity modes, respectively.

using Eqs. (1), (3), and (4). We again consider a Gaussian pulse with the electric field in Eq. (12), but its width is much larger than the round-trip time of 0.23 ps ($T_0 = 10$ ps). The facet reflectivity is increased to 98.2% to ensure a relatively large value of photon lifetime (6.5 ps). The input frequency of 192.86 THz is again chosen to be on resonance with a cavity mode. To make our results more relevant to experiments, the refractive index is decreased by only 0.1% from its initial value of 3.5. Moreover, we do not assume this change to be instantaneous but consider the situation in which refractive index is decreased linearly over a time interval starting at $T_i = 3$ ps to the final time $T_f = 6$ ps (the origin of time is at the peak of the input pulse).

The pulse shapes and spectra are plotted in Figs. 5(a) and 5(b), respectively for the input (black dashed curve), static-case output (green dotted curve), and dynamic-case output (red solid curve). A comparison of the green and red curves reveals the impact of the 0.1% index change on the output pulse. Consider the spectral changes first. As depicted in Fig. 5(b), the output spectrum shows a new peak shifted toward higher frequencies. This peak represents the AWC expected because the resonant frequencies of the cavity modes shift toward the blue side by about 190 GHz after the index change has been completed. Indeed, the central frequency of this shifted peak agrees well with the new position of the resonator modes. The amplitude of the shifted peak is larger than that at the original frequency, indicating that a large portion of the pulse energy has shifted to the new resonator mode.

The reason that some energy is still left at the original resonator mode is related to the fact that the entire pulse does not experience the index change. A portion of the front part of the pulse leaves the resonator before the refractive index begins to change. Similarly, a portion of the back part of the pulse enters the medium after the index change has occurred. Because this part is no longer in resonance with the shifted cavity mode, its coupling into the resonator is reduced. The

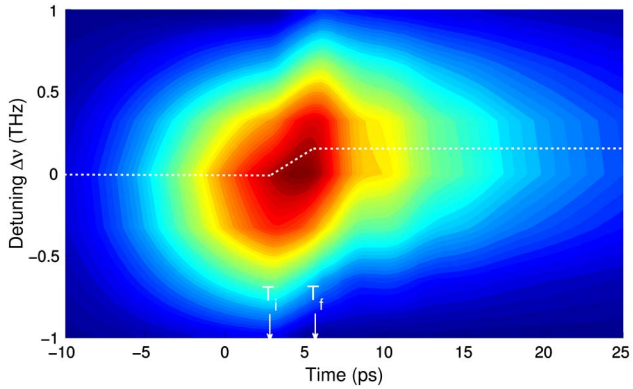


Fig. 6. (Color online) Spectrogram for the long-pulse case shown in Fig. 5. The pulse spectrum appears to follow the cavity resonance indicated by the dotted line.

time dependence of the output spectrum is better revealed in the spectrogram shown in Fig. 6, where the pulse spectrum appears to follow the temporal changes in the refractive index. Note that some pulse energy also lies in between the original and shifted resonator modes. This energy comes from the part of the pulse that only experiences a fraction of the index change (i.e., parts of the pulse that either leave or enter the resonator during the index change).

Figure 5(a) reveals significant changes in the output pulse shape introduced by the dynamic index changes taking place inside the FP resonator. The peak of the output pulse (solid red curve) occurs close to the front of the pulse when compared to the static case (dotted green curve). This temporal behavior occurs because index changes shift the mode frequencies of the resonator, which makes the trailing part of the pulse to be off resonance. This shifting explains the considerable reduction in the energy contained in the trailing part the output pulse. In addition, we also see an evidence of oscillations (period of about 5 ps) of decreasing amplitude just after the index change has been completed (the kneelike feature). We interpret these oscillations as resulting from beating of light at the shifted frequency with light at the original frequency.

## 5. VARIATION OF CONTROLLABLE PARAMETERS

The results presented in Section 4 show that dynamic changes in the refractive index of an FP resonator produce an AWC peak during transmission of an optical pulse, but they also lead to several other temporal and spectral changes in the output pulse. In the time domain, pulses become asymmetric and their width may increase or decrease depending on the direction in which the refractive index is changed. In the spectral domain, output spectra develop a multipeak structure and are distorted considerably in an asymmetric fashion. In addition, pulses develop considerable frequency chirp. The magnitude of these changes depends considerably on various factors that can be controlled during an experiment. In this section, we explore three such factors related to the temporal duration over which the index change is completed: the speed and the magnitude of the index change and detuning of the input wavelength from the nearest FP resonance.

### A. Speed of Index Change

The word "adiabatic" in AWC requires that refractive-index changes occur slower than some characteristic time. In the case of an optical field, the shortest characteristic time is the optical period. However, a second, much-longer time scale, the photon lifetime, is also relevant for optical resonators. If the refractive index is changed slowly over a long duration, not much pulse energy is likely to remain in the resonator after the index change has been completed. The important question is how much the shape and spectrum of the output pulse depend on the speed of index change. To answer this question, we consider again transmission of 10 ps Gaussian pulses through the same FP resonator used for Fig. 5 but allow the temporal duration, $T_f - T_i$, over which the index is reduced linearly by 0.1%, to vary from 3 to 27 ps. Figure 7 shows the shape and spectrum of output pulses for three choices of $T_f$ while fixing all other parameters (initial time, pulse width, and magnitude of index change) to their same values used in Fig. 5. In all cases, the photon lifetime is fixed at 6.5 ps. Changes in the pulse shape are easily understood once we interpret the spectral modifications correctly.

When the refractive index change is completed well within the photon lifetime ($T_{f1} - T_i = 3$ ps, dashed red curve), the new AWC peak dominates the pulse spectrum, as its amplitude is larger than that of the peak at the original mode frequency. However, as the duration of index change becomes larger than the photon lifetime ($T_{f2} - T_i = 13$ ps, dotted–dashed blue curve), the amplitude of the AWC peak is reduced considerably. Much more pulse energy remains at the original mode frequency, and considerable pulse energy lies in between the two modes. When the duration of the index change is increased further to $T_{f3} - T_i = 27$ ps (solid purple curve), the AWC peak almost disappears as little energy of the pulse appears at the shifted mode frequency. Note, however, that the pulse spectrum is distorted considerably even in this case: it is broader and highly asymmetric compared to the static case. The reason is that spectral broadening occurs only toward the blue side, which is expected when the refractive

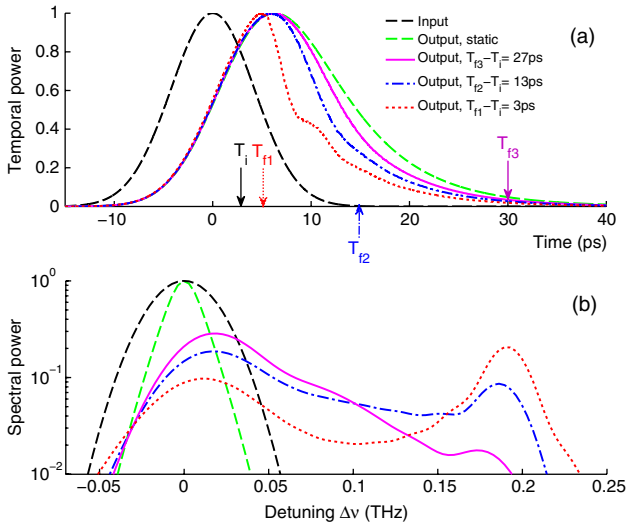


Fig. 7. (Color online) Impact of index-change duration $\Delta T = T_f - T_i$ on propagation of 10 ps Gaussian pulses in the case of a −0.1% linear change in the refractive index beginning at $T_i = 3$ ps. (a) Output pulse narrows down and exhibits oscillations as $\Delta T$ decreases. (b) Amplitude of the AWC peak also increases as $\Delta T$ decreases.

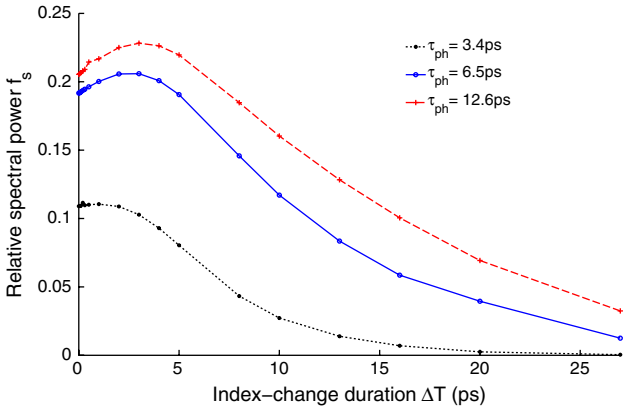


Fig. 8. (Color online) AWC efficiency as a function of index-change duration $\Delta T$ for three values of photon lifetimes $\tau_{\mathrm{ph}}$ in the case of $\Delta n = -0.1\%$. The efficiency is maximum for $\Delta T$ near zero when $\tau_{\mathrm{ph}}$ is relatively small, but it peaks at a value of $\Delta T > 0$ that increases with $\tau_{\mathrm{ph}}$.

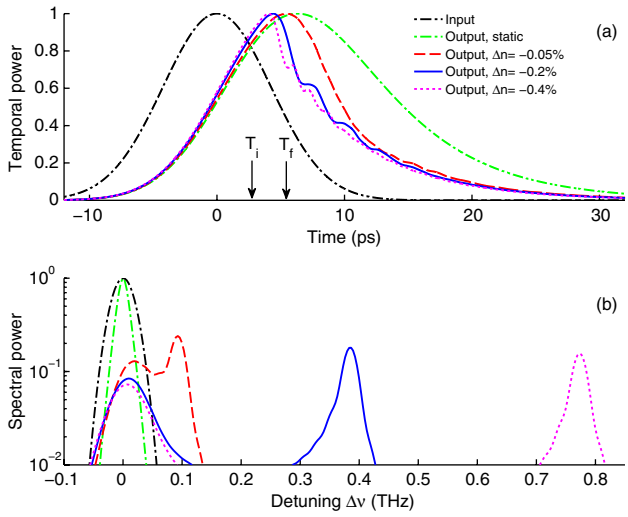


Fig. 9. (Color online) Impact of the magnitude of $\Delta n$ for a fixed linear index-change duration of 3 ps, input pulse width of 10 ps, and a round-trip time of 0.23 ps. (a) The oscillation frequency in the pulse tail increases for a larger index change because of (b) a larger AWC-induced shift in the mode frequency.

index is reduced from its original value and cavity modes experience a blueshift.

The efficiency of the AWC process can be characterized by a parameter $f_s$ representing the power of the AWC peak relative to the input peak. Physically, $f_s$ represents the fraction of pulse energy that is contained within the AWC peak. This quantity is plotted by the solid blue curve in Fig. 8 for the FP resonator used in Fig. 5, which has a photon lifetime of $\tau_{\mathrm{ph}} = 6.5$ ps, as a function of the duration $\Delta T = T_f - T_i$ over which index changes are completed. The value $\Delta T = 0$ corresponds to an instantaneous change discussed in Section 3. Note that $f_s$ increases slightly in the range of $\Delta T = 0$ to 3 ps, where it reaches its peak value of about 21%. Beyond that, $f_s$ displays a monotonic decay as $\Delta T$ increases further. The initial increase at up to $\Delta T = 3$ ps results from a relatively long duration of the input pulse. When the refractive index begins to change, the energy is still being injected into the resonator, and the energy inside the resonator reaches its maximum just before the index change is completed for $\Delta T = 3$ ps, resulting in an optimum situation. The monotonic decay beyond that is characterized by the continuously decreasing fraction of pulse energy that enters the resonator after the index changes have been completed. Also shown in Fig. 8 are the $f_s$ for two other resonators with different values of photon lifetime $\tau_{\mathrm{ph}}$: 3.4 and 12.6 ps for the dotted black and dashed red curves, respectively. Note the three resonators shown in Fig. 8 are identical, expect for their mirror reflectivity (96.5%, 98.2%, and 99% for the black, blue, and red cases, respectively).

Our model not only correctly confirms the previous understanding on AWC that the index change has to happen within the photon lifetime of the cavity [3–5], but it also shows that the optimum situation does not correspond to an instantaneous index change. In fact, we predict that a slower index change is better for improving the AWC efficiency in resonators with relatively long photon lifetimes.

### B. Magnitude of Index Change

In the previous discussion, we used a fixed value of −0.1% for the relative index change. The impact of magnitude of relative refractive-index change $\Delta$, defined from $n_2 = n_1(1 - \Delta)$, is studied in this subsection. Figure 9 shows the shape and spectrum of output pulses by changing this value in the range of 0.05% to 0.4%, while keeping all other parameters identical to those used for Fig. 5. In particular, $T_f - T_i = 3$ ps in all cases. Pulse shapes in part (a) are affected much less by changes in $\Delta$ compared with the spectral changes. Changes in frequency or wavelength are linearly proportional to the index change. As seen in Fig. 9(b), the AWC-induced spectral shift increases from 95 to 760 GHz as $\Delta$ increases from 0.05% to 0.4%. This behavior agrees with previous studies on AWC [3,4]. The magnitude of the AWC peak does not depend on $\Delta$ much, and it appears to saturate for $\Delta > 0.2\%$. The larger magnitude of this peak for $\Delta = 0.05\%$ results from an overlapping of the original and shifted peaks for such small index changes.

As far as changes in the pulse shape are concerned, we note from Fig. 9(a) that the pulse peak occurs closer to the front side as $\Delta$ increases. As already discussed, this shift is a consequence of the trailing part of the pulse falling out of resonance after the index change has occurred. Notice also an increase in the frequency of oscillations in the trailing part of the pulse as $\Delta$ increases. This behavior is understandable by recalling that the oscillation frequency is equal to the spectral shift induced by the AWC process, which itself increases with $\Delta$ rapidly, as seen in Fig. 9(b). For $\Delta = 0.2\%$ one can see four oscillation cycles with a period of about 2.5 ps, which agrees with a spectral shift of 0.4 THz. The oscillation period is reduced to near 1.2 ps for $\Delta = 0.4\%$ because of a doubling of the AWC-induced frequency shift. The number of oscillations is set by the time interval over which the resonator contains light at both the original and shifted mode frequencies. In the case of $\Delta = 0.4\%$, almost all of pulse energy within the resonator shifts to the new mode frequency after four cycles.

### C. Detuning of Input Frequency

So far we have assumed that the carrier frequency (or the launch wavelength) of the input pulse coincides with one of the modes of the resonator. This was also the situation in most experiments [4,5], and it is often argued that an on-resonance pulse launch is required for AWC to occur. The effect of input frequency detuning was studied experimentally in [4], showing that less light is converted as the input is

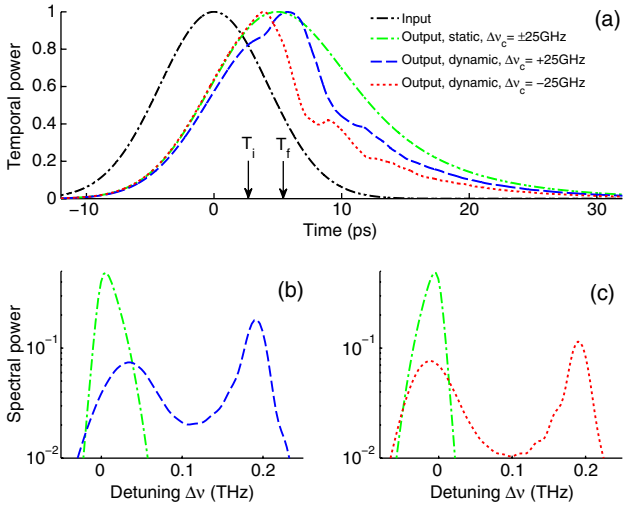


Fig. 10. (Color online) Impact of detuning $\Delta\nu_c$ of the input pulse from a cavity resonance ($\Delta\nu_c = \nu_0 - \nu_c$, where $\nu_0$ and $\nu_c$ are the input carrier frequency and cavity-resonance frequency, respectively) for a $-0.1\%$ linear change in the refractive index between $T_i = 3$ ps and $T_f = 6$ ps (the round-trip time is 0.23 ps). (a) Output pulse shapes show an asymmetry with respect to the sign of $\Delta\nu_c$. (b) The amplitude of the AWC peak is larger for a $+25$ GHz detuning than for the $-25$ GHz detuning (in this negative index-change case).

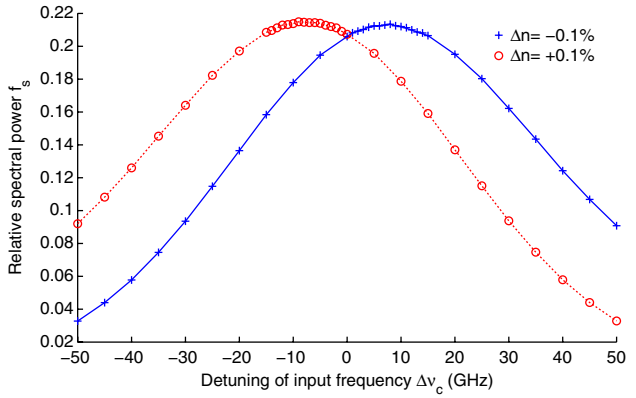


Fig. 11. (Color online) Fraction of pulse energy transferred to the AWC peak as a function of detuning of input pulse from a cavity resonance under the same long-pulse conditions as in Fig. 10 but for an index change of $-0.1\%$ (blue solid curve) and $+0.1\%$ (red dotted curve).

detuned from resonance. In this subsection we consider off-resonance launching of input pulses. Figure 10 shows the shape and the spectrum of output pulses when the 10 ps Gaussian pulse is detuned from resonance by $\pm 25$ GHz. All other parameters are kept identical to those in Fig. 5. In particular, $\Delta = 0.001$ and $T_f - T_i = 3$ ps. It is evident from Fig. 10 that all qualitative spectral and temporal features that occur when input pulse is on-resonance also occur in the off-resonance case with minor modifications.

A new feature that is apparent in Fig. 10(a) is related to the direction in which the peak of the output pulse moves in a dynamic resonator compared to the static case (green curve). More specifically, the pulse peak shifts toward or away from the leading edge depending on whether the detuning $\Delta\nu_c$ is $-25$ GHz or $+25$ GHz. The can be understood by noting that the cavity resonance moves toward the blue side in both cases (because of a negative index change). If the pulse is initially detuned on the red side of the resonance peak, a larger portion of its trailing part will experience reduced transmittance compared to when the pulse is initially detuned on the blue side. The oscillation frequency is different in the two cases because the beat frequency between the original and shifted peaks is different (about 140 and 200 GHz) as seen from the spectra in parts (b) and (c).

The relative power of the AWC peak is larger in the case of positive detuning $\Delta\nu_c$ (case b in Fig. 10) compared to the case of negative detuning (case c). This can also be understood from the blueshift of the AWC peak in the case of a negative index change. The opposite would happen if the index were increased and the AWC peak were shifted toward the red side of the original peak. This behavior is shown more clearly in Fig. 11 by plotting the relative power $f_s$ of the AWC peak as a function of input detuning. A somewhat surprising feature of this figure is that, contrary to the conventional wisdom, the maximum energy transfer to the AWC peak does not occur under on-resonance conditions. Clearly, if the objective is to transfer as much pulse energy as possible to the AWC peak, one should detune the input pulse carrier frequency in the same direction in which the resonator mode is expected to shift after changes in the refractive index have been completed.

## 6. CONCLUDING REMARKS

We present a simple and intuitive model based on the impulse response of linear systems for describing the propagation of optical pulses through a dynamic FP resonator, containing a linear medium whose refractive index changes with time. Our model is based on how the transit time of different slices of the launched pulse is affected by time-dependent index changes. It shows that the adiabatic wavelength shift results from a scaling of the slice transit time by a factor that depends on both the magnitude and sign of the index change. We apply our general theory first to the case in which pulses that are short compared with the round-trip time are transmitted, and the refractive index of the resonator is changed instantaneously after a pulse has been launched. We obtain an analytic form of the resonator output in this situation.

The case of pulses longer than the round-trip time is discussed in detail, as it is expected to be more relevant experimentally. We consider transmission of picosecond Gaussian pulses through a 10 $\mu$m long FP resonator and allow the refractive index of the resonator to change over a duration ranging from 3 to 30 ps. The magnitude of index change also varies between 0% to 0.4%. We show that an adiabatic wavelength shift is always accompanied by significant changes in both the shape and the spectrum of output pulses. We discuss in detail how such temporal and spectral changes depend on externally controllable parameters such as the magnitude and the speed of the index change and detuning of the input pulse from the cavity resonance. Our result should find applications in the area of optical signal processing with resonant photonic structures based on microrings or photonic crystals.

## ACKNOWLEDGMENTS

This work is supported in part by the National Science Foundation (NSF) under award ECCS-1041982.

## REFERENCES


1. M. F. Yanik and S. Fan, "Stopping light all optically," Phys. Rev. Lett. **92**, 083901 (2004).
2. M. F. Yanik and S. Fan, "Time reversal of light with linear optics and modulators," Phys. Rev. Lett. **93**, 173903 (2004).
3. M. Notomi and S. Mitsugi, "Wavelength conversion via dynamic refractive index tuning of a cavity," Phys. Rev. A **73**, 051803 (2006).
4. S. Preble, Q. Xu, and M. Lipson, "Changing the colour of light in a silicon resonator," Nat. Photon. **1**, 293–296 (2007).
5. T. Tanabe, M. Notomi, H. Taniyama, and E. Kuramochi, "Dynamic release of trapped light from an ultrahigh-*Q* nanocavity via adiabatic frequency tuning," Phys. Rev. Lett. **102**, 043907 (2009).
6. Z. Gaburro, M. Ghulinyan, F. Riboli, and L. Pavesi, "Photon energy lifter," Opt. Express **14**, 7270–7278 (2006).
7. S. E. Harris and O. P. McDuff, "Theory of FM laser oscillation," IEEE J. Quantum Electron. **1**, 245–262 (1965).
8. M. J. Lawrence, B. Willke, M. E. Husman, E. K. Gustafson, and R. L. Byer, "Dynamic response of a Fabry–Perot interferometer," J. Opt. Soc. Am. B **16**, 523–532 (1999).
9. M. Rakhmanov, "Doppler-induced dynamics of fields in Fabry–Perot cavities with suspended mirrors," Appl. Opt. **40**, 1942–1949 (2001).
10. H. Rohde, J. Eschner, F. Schmidt-Kaler, and R. Blatt, "Optical decay from a Fabry–Perot cavity faster than the decay time," J. Opt. Soc. Am. B **19**, 1425–1429 (2002).
11. D. Redding, M. Regehr, and L. Sievers, "Dynamic models of Fabry–Perot interferometers," Appl. Opt. **41**, 2894–2906 (2002).
12. M. Rakhmanov, R. L. Savage, D. H. Reitze, and D. B. Tanner, "Dynamic resonance of light in Fabry–Perot cavities," Phys. Lett. A **305**, 239–244 (2002).
13. T. Kampfrath, D. M. Beggs, T. P. White, A. Melloni, T. F. Krauss, and L. Kuipers, "Ultrafast adiabatic manipulation of slow light in a photonic crystal," Phys. Rev. A **81**, 043837 (2010).
14. Y. Xiao, G. P. Agrawal, and D. N. Maywar, "Spectral and temporal changes of optical pulses propagating through time-varying linear media," Opt. Lett. **36**, 505–507 (2011).
15. G. P. Agrawal, *Lightwave Technology: Components and Devices* (Wiley, 2004).
16. G. P. Agrawal, *Nonlinear Fiber Optics*, 4th ed. (Academic, 2007).